Reply to reviewer #2

This manuscript presents a comprehensive dataset of satellite-derived NO_x emissions over China for 2019–2024, based on an enhanced Directional Derivative Approach (DDA). The resulting dataset is spatially resolved, covers both regional and point-source emissions, and is validated against multiple bottom-up inventories and independent top-down products. The work is clearly within the scope of ESSD. Overall, the manuscript is well written and supported by extensive analysis. However, several methodological assumptions require further clarification. I therefore recommend publication after these revisions. The paper is generally well written and should be published after dealing with the following issues:

We are grateful to the reviewer for the positive assessment of our manuscript and for the constructive comments on the methodological assumptions. We have carefully addressed all comments and revised the manuscript accordingly. Detailed point-by-point responses are provided below, with our replies shown in blue and all revisions highlighted in italics.

Method and results:

1. Please explicitly state the TROPOMI NO_2 product version used in the proposed method.

Response: The operational offline TROPOMI NO_2 TVCD product (S5P_L2__NO2___HiR2) from NASA GES DISC is used in this study. As discussed in Line 494–496, this work primarily aims to propose a practical and insightful perspective for addressing nonlinear NO_x chemistry in emissions estimation, rather than focusing on improvements in retrieval data quality (e.g., air mass factor corrections in satellite NO_2 retrievals). The standard operational NO_2 product is selected, and additional corrections are expected to improve estimation accuracy. We added a brief clarification **in Lines 94–95**: *The operational offline TROPOMI NO_2 TVCD product (S5P_L2__NO2___HiR2) (Van Geffen et al., 2024) from NASA GES DISC (https://daac.gsfc.nasa.gov/datasets/) for 2019–2024 is used in this study.*

2. The piecewise fitting of NO_x lifetime as a function of NO_2 TVCD percentile and subregion (Sect. 3.2) is a key innovation of this work. Please provide additional information on: The minimum number of grid cells per bin used for fitting and Whether a smoother functional form (rather than piecewise bins) was tested. A clearer discussion would strengthen the methodological transparency.

Response: NO_x lifetime is fitted for each individual month and subsequently averaged for the same month within each subregion over the study period. After data retrieval and fitting threshold filtering, a total of 1393 month-bins are successfully fitted across the four subregions. The number of grid cells per bin ranges from 3 to 9388 (10^{th} percentile: 17; median: 91; mean: 199), indicating that most bins contain sufficient data for robust lifetime fitting, while bins with very small sample sizes are rare and have negligible influence on the overall regression. The mean lifetime for each month-bin is calculated by averaging the successfully fitted bins across all years. The number of grid cells contributing to each month-bin mean ranges from 8 to 38,610 (10^{th} percentile: 67; median: 382; mean: 789). We added the values **in Lines 221–224**: *A total of 1393 month-bins are successfully fitted across the four subregions. The number of grid cells per bin ranges from 3 to 9388 (10^{th} percentile: 17; median: 91; mean: 199), indicating that most bins contain sufficient data for robust lifetime fitting, while bins with very small sample sizes are rare and have negligible influence on the overall regression.*

NO_x lifetime first increases at very low NO_x concentrations, then decreases at moderate levels, and

can rise again at very high NO_x due to the "NO_x-suppressed" regime (Lange et al., 2022; Pusede et al., 2015). This nonlinear behavior is difficult to describe with a single smooth function. The piecewise fitting scheme combines multiple linear fits across NO_2 TVCD bins, using the NO_x concentrations that affect lifetime as references while accounting for regional background conditions, providing a simple and robust approach to represent nonlinear NO_x chemistry in the DDA framework. We added a brief discussion **in Lines 462–463**: *This scheme combines multiple linear fits based on NO_2 TVCD levels, providing a simple and robust way to represent nonlinear NO_x chemistry in the DDA framework.*

3. Please quantify how national anthropogenic totals change under alternative assumptions (e.g., different NTL thresholds or without subtracting soil emissions). This will help users better interpret the dataset.

Response: We added **Table S2 and Figure S6 in the Supplement** to support the choice of the NTL threshold. The results indicate that without applying the NTL constraint, anthropogenic NO_x emissions would be underestimated by 5.4–15.1%. In contrast, the differences among results obtained with different NTL thresholds are relatively small (−4.9% to 3.6%). Furthermore, if soil and biomass burning NO_x emissions from grids not classified as natural sources are not subtracted using the inventory, anthropogenic NO_x emissions would be overestimated.

The corresponding discussion has been added **in Lines 367–378** as follows: *Table S2 shows NO_x emissions from sensitivity tests of the anthropogenic NO_x filter threshold, and Figure S6 presents the probability density function (PDF) of nighttime light (NTL) to support the selection of the NTL threshold. The results indicate that without applying the NTL constraint, anthropogenic NO_x emissions would be underestimated. The differences among results obtained with different NTL thresholds are relatively small (−4.9% to 3.6%). Under the selected threshold of 0.01 nW cm^{-2} sr^{-1}, more than 90% of NTL grids are identified as anthropogenic sources, and this threshold also helps minimize the resampling effect from 500 m to 0.05° in dark regions. Overall, the small differences among different thresholds and the good agreement with other datasets demonstrate the robustness of the anthropogenic NO_x source filtering approach used in this study.*

Table S2. NO_x emissions from sensitivity tests of the anthropogenic NO_x filter threshold.

This work (NTL_0.01): Grid cells with either the highest averaged NO_2 TVCDs in summer or the lowest values in winter comparing to other seasons, and with NTL < 0.01 nW cm^{-2} sr^{-1}, are subtracted as natural NO_x (NO_x_nat), and for the remaining grid cells, soil and biomass burning emissions (from CAMS data) are further subtracted to obtain anthropogenic NO_x (NO_x_anthro);

NTL_none: Same as this work, but without applying the NTL filter;

NTL_0.00: Same as this work, but with NTL = 0.00 nW cm^{-2} sr^{-1};

NTL_0.05: Same as this work, but with NTL < 0.05 nW cm^{-2} sr^{-1};

CAMS_none: Same as this work, but soil and biomass burning emissions from CAMS data are not subtracted;

NTL_anthro: Fraction of NTL grids that are also classified as anthropogenic NO_x grids.

Year	*Variable*	*Test*				
		This work (NTL_0.01)	*NTL_none*	*NTL_0.00*	*NTL_0.05*	*CAMS_none*
2019	*NO_x_anthro (Tg)*	*20.2*	*18.9*	*20.7*	*19.7*	*21.3*
	NO_x_nat (Tg)	*9.6*	*11.0*	*9.2*	*10.1*	*9.6*
	NTL_anthro (%)	*93.0*	*77.4*	*100.0*	*85.5*	*93.0*

	NO_x_anthro (Tg)	*18.5*	*17.3*	*18.9*	*18.1*	*19.6*
2020	*NO_x_nat (Tg)*	*10.3*	*11.5*	*9.9*	*10.7*	*10.3*
	NTL_anthro (%)	*93.5*	*78.1*	*100.0*	*86.7*	*93.5*
	NO_x_anthro (Tg)	*19.4*	*18.3*	*19.7*	*19.0*	*20.5*
2021	*NO_x_nat (Tg)*	*9.3*	*10.4*	*9.0*	*9.7*	*9.3*
	NTL_anthro (%)	*94.1*	*81.6*	*100.0*	*88.1*	*94.1*
	NO_x_nat (Tg)	*18.9*	*17.2*	*19.4*	*18.3*	*20.0*
2022	*NO_x_nat (Tg)*	*9.3*	*11.0*	*8.8*	*9.9*	*9.3*
	NTL_anthro (%)	*93.2*	*74.7*	*100.0*	*85.0*	*93.2*
	NO_x_anthro (Tg)	*20.7*	*17.7*	*21.3*	*19.8*	*21.8*
2023	*NO_x_nat (Tg)*	*8.1*	*11.0*	*7.4*	*9.0*	*8.1*
	NTL_anthro (%)	*92.6*	*66.9*	*100.0*	*83.0*	*92.6*
	NO_x_anthro (Tg)	*18.8*	*16.0*	*19.5*	*17.9*	*19.9*
2024	*NO_x_nat (Tg)*	*8.5*	*11.4*	*7.9*	*9.5*	*8.5*
	NTL_anthro (%)	*92.0*	*67.4*	*100.0*	*82.0*	*92.0*

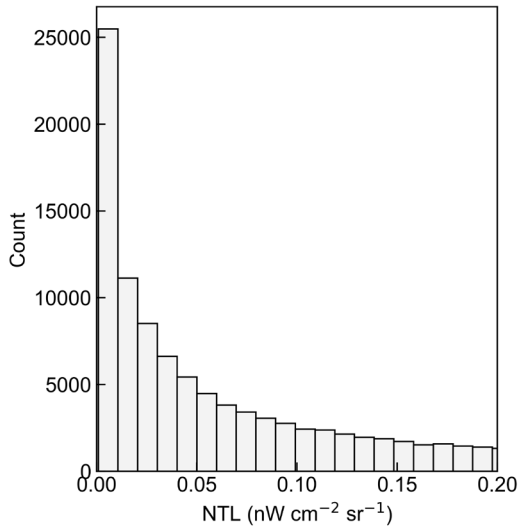

Figure S6. Probability density function (PDF) of SNPP/VIIRS Nighttime Light (NTL) in China in 2023.

4. Line 22–24: "first application of a lightweight, satellite-driven method" — please clarify "first" relative to previous DDA/FDA-based studies (e.g., Beirle et al., Ayazpour et al.).

Response: Two key challenges remain for NO_x emission estimation using the FDA and DDA, including the NO_x/NO_2 ratio and the nonlinear NO_x lifetime. Previous studies have accounted for spatial variability of NO_x/NO_2 ratios using auxiliary data (Beirle et al., 2021, 2023; Ayazpour et al., 2025; Cifuentes et al., 2025; Meier et al., 2024) and explored factors (Beirle et al., 2023; Lange et al., 2022; Krol et al., 2024; Meier et al., 2024) to represent lifetime variability. However, capturing nonlinear NO_x chemistry (Laughner and Cohen, 2019) remains difficult (in Lines 70–84). As a result, estimated emissions often contain a considerable number of negative grids due to imbalances among local emissions, horizontal transport, and chemical loss, limiting the applicability of lightweight methods when extending from point sources (Beirle et al., 2019, 2021, 2023; Sun, 2022) or individual cities (Cifuentes et al., 2025; Lonsdale and Sun, 2023) to regional emission estimation (in Lines 276–279 and 506–513).

In this work, by incorporating a spatially variable NO_x/NO_2 ratio and implementing a data-driven, piecewise fitting strategy, we extend the lightweight satellite-based DDA framework to estimate both point-source and regional NO_x emissions across China. In this context, "first" refers to *the application of a lightweight, satellite-driven NO_x emissions estimator in such a large and topographically complex region* (in Lines 19–21 and 511–513).

5. Line 114–118: Justify the use of near-surface NO_x/NO_2 ratios for column-based inversion more explicitly.

Response: We revised the manuscript for clarity **in Lines 112–116**: *The NO_x/NO_2 ratios are highest near emission sources because freshly emitted NO rapidly consumes local ozone and is subsequently oxidized to NO_2 as the plume mixes with background air (Meier et al., 2024). Following Beirle et al. (2021, 2023), NO_2 columns are converted to NO_x using the near-surface photostationary state, with the NO_x/NO_2 ratio from the near-surface model layer with a 1-hour temporal resolution (chm_tavg_1hr_g1440x721_v1) used in this study to better represent near-source conditions and the resulting NO_x gradients (Ayazpour et al., 2025; Sun, 2022).*

6. Eq. (1)–(2): Please define all vector operators and clarify notation for gradients (horizontal or terrain-following).

Response: In Eqs. (1)–(2), ∇ denotes the two-dimensional horizontal vector differential operator in Cartesian coordinates, i.e., $\nabla = (\partial/\partial x, \partial/\partial y)$, No terrain-following coordinate system is used in this formulation. The operator $\langle\rangle$ denotes spatiotemporal averaging. These clarifications have been added to the revised manuscript **in Lines 153–154 and 162**.

7. Line ~223: Clarify whether bins are constructed independently for each month or based on climatological distributions.

Response: We revised the manuscript for clarity **in Lines 212–215**: *Given the small interannual variability and limited impact on reactive species emission estimation (Ayazpour et al., 2025), β_1 is fitted using the same climatological months, whereas β_2 is fitted for each individual month using NO_2 TVCD percentile bins constructed independently for that month and subsequently averaged over the same months for each subregion during 2019–2024.*

8. Line ~495–500: Lifetime ranges reported here differ slightly from Sect. 4.2; please ensure consistency.

Response: We thank the reviewer for pointing this out. We have corrected the discrepancy, and the lifetime ranges are now consistent with those reported in Sect. 4.2.

9. Please clarify whether σ_0 (Eq. 7) includes satellite retrieval noise or only directional variability in DDF.

Response: σ_0 in Fig. 2 is estimated from the standard deviation of the difference between $DDf_{\vec{x}/\vec{y}}$ and $DDf_{\vec{r}/\vec{s}}$, based on 0.05° grids by resampling satellite orbit data. As such, σ_0 inherently includes both the satellite retrieval noise and the random error associated with the DDF estimator (directional variability). We revised the description **in Lines 263–265** as follows: *Therefore, the random error of DDf is employed to characterize the uncertainties in DDA emission estimation, encompassing both satellite retrieval noise and the random error arising from the DDf estimator.*

Dataset:

10. The public availability of the data via Zenodo is strongly appreciated and fully aligns with the mission of Earth System Science Data. Please expand the data description (Sect. 6 or Supplement) to include: A table listing all variables, units, dimensions, and fill values. Explicit statement of whether emissions are reported as NO_2-equivalent mass or NO_x mass.

Response: We added a data description as **Table S3 in the Supplement**.

Table S3. Description of variables in the dataset.

Name	*Description*	*Dimensions*	*Units*	*Fill_value*
lat	*Latitude*	*lat*	*degrees_north*	*NaN*
lon	*Longitude*	*lon*	*degrees_east*	*NaN*
grid_area	*Grid-cell area*	*lat × lon*	m^2	*NaN*
NO_x_emission	*Annual anthropogenic NO_x emissions per grid*	*lat × lon*	*tonnes (1 tonne =10^3 kg)*	*NaN*

As noted by the reviewer, we clarify this issue **in Lines 178–179** as follows: *All bracketed terms are averaged at a monthly scale before X and τ are fitted (see in Sect. 3.2) to derive emissions (EE) in mol m^{-2} s^{-1}, and the conversion to mass assumes NO_x as NO_2.*

11. Please clarify whether grid-level or regional uncertainty fields are included in the data files. If not, whether uncertainty estimates are provided at aggregated scales only (e.g., national/provincial).

Response: Grid-level uncertainties are not included in the NetCDF data files, because the regional uncertainties are calculated by aggregating grid-level precision according to Eq. (3). Instead, aggregated uncertainty estimates at national and point-source scales and are added in a separate Excel file (**NOx_national_pointsource_2019_2024.xlsx**).

12. The manuscript notes that the improved fitting scheme reduces negative emission artifacts, but it is unclear how such values are handled in the final dataset. Whether negative grid-cell emissions are retained, masked, or truncated in the released data.

Response: All negative grid-cell emissions are retained in the dataset without masking or truncation to preserve the original inversion results.

13. Please clarify whether future updates (e.g., extension beyond 2024 or revised inputs) are planned.

Response: We plan to extend the dataset beyond 2024 and release updated versions as needed, which will be shared through the same platform.

The updated dataset (Version 1.1) is available at https://doi.org/10.5281/zenodo.18923337 (Chen et al., 2026).

We sincerely thank the reviewer again for the helpful comments that improved both the manuscript and the dataset, as well as for the interest and encouragement regarding the continued development of this method.

References

Ayazpour, Z., Sun, K., Zhang, R., and Shen, H.: Evaluation of the Directional Derivative Approach for Timely and Accurate Satellite-Based Emission Estimation Using Chemical Transport Model Simulation of Nitrogen Oxides,

Journal of Geophysical Research: Atmospheres, 130, e2024JD042817, https://doi.org/10.1029/2024JD042817, 2025.

Beirle, S., Borger, C., Dörner, S., Li, A., Hu, Z., Liu, F., Wang, Y., and Wagner, T.: Pinpointing nitrogen oxide emissions from space, Sci. Adv., 5, eaax9800, https://doi.org/10.1126/sciadv.aax9800, 2019.

Beirle, S., Borger, C., Dörner, S., Eskes, H., Kumar, V., De Laat, A., and Wagner, T.: Catalog of NO_x emissions from point sources as derived from the divergence of the NO_2 flux for TROPOMI, Earth Syst. Sci. Data, 13, 2995–3012, https://doi.org/10.5194/essd-13-2995-2021, 2021.

Beirle, S., Borger, C., Jost, A., and Wagner, T.: Improved catalog of NO_x point source emissions (version 2), Earth Syst. Sci. Data, 15, 3051–3073, https://doi.org/10.5194/essd-15-3051-2023, 2023.

Chen, L., Cai, Z., Sun, K., Liu, Y., Yang, D., Li, M., and Zhu, L.: Regional and point source nitrogen oxides emissions in China from TROPOMI, https://doi.org/10.5281/zenodo.18923337, 2026.

Cifuentes, F., Eskes, H., Dammers, E., Bryan, C., and Boersma, F.: Accurate space-based NO_x emission estimates with the flux divergence approach require fine-scale model information on local oxidation chemistry and profile shapes, Geoscientific Model Development, 18, 621–649, https://doi.org/10.5194/gmd-18-621-2025, 2025.

Lange, K., Richter, A., and Burrows, J. P.: Variability of nitrogen oxide emission fluxes and lifetimes estimated from Sentinel-5P TROPOMI observations, Atmospheric Chemistry and Physics, 22, 2745–2767, https://doi.org/10.5194/acp-22-2745-2022, 2022.

Laughner, J. L. and Cohen, R. C.: Direct observation of changing NO_x lifetime in North American cities, Science, 366, 723–727, https://doi.org/10.1126/science.aax6832, 2019.

Lonsdale, C. R. and Sun, K.: Nitrogen oxides emissions from selected cities in North America, Europe, and East Asia observed by the TROPOspheric Monitoring Instrument (TROPOMI) before and after the COVID-19 pandemic, Atmos. Chem. Phys., 23, 8727–8748, https://doi.org/10.5194/acp-23-8727-2023, 2023.

Meier, S., Koene, E. F. M., Krol, M., Brunner, D., Damm, A., and Kuhlmann, G.: A lightweight NO_2-to-NO_x conversion model for quantifying NO_x emissions of point sources from NO_2 satellite observations, Atmospheric Chemistry and Physics, 24, 7667–7686, https://doi.org/10.5194/acp-24-7667-2024, 2024.

Pusede, S. E., Steiner, A. L., and Cohen, R. C.: Temperature and Recent Trends in the Chemistry of Continental Surface Ozone, Chem. Rev., 115, 3898–3918, https://doi.org/10.1021/cr5006815, 2015.

Sun, K.: Derivation of Emissions From Satellite-Observed Column Amounts and Its Application to TROPOMI NO_2 and CO Observations, Geophysical Research Letters, 49, e2022GL101102, https://doi.org/10.1029/2022GL101102, 2022.